SCIENTIFIC REPORTS

OPEN

SUBJECT AREAS:
BIOCHEMISTRY
ELECTROCHEMISTRY

Received
20 March 2014

Accepted
15 May 2014

Published
9 June 2014

Correspondence and requests for materials should be addressed to K.H.B. (keith.baronian@canterbury.ac.nz)

Electrochemical detection of intracellular and cell membrane redox systems in *Saccharomyces cerevisiae*

Frankie J. Rawson[1,2], Alison J. Downard[2,3] & Keith H. Baronian[4]

[1]Laboratory of Biophysics and Surfaces Analysis, School of Pharmacy, University of Nottingham, University Park, Nottingham B15 2TT UK, [2]Department of Chemistry, University of Canterbury, Private Bag 4800, Christchurch, New Zealand, [3]MacDiarmid Institute for Advanced Materials and Nanotechnology, University of Canterbury, Private Bag 4800, Christchurch, New Zealand, [4]School of Biological Sciences, University of Canterbury, Private Bag 4800, Christchurch, New Zealand.

Redox mediators can interact with eukaryote cells at a number of different cell locations. While cell membrane redox centres are easily accessible, the redox centres of catabolism are situated within the cytoplasm and mitochondria and can be difficult to access. We have systematically investigated the interaction of thirteen commonly used lipophilic and hydrophilic mediators with the yeast *Saccharomyces cerevisiae*. A double mediator system is used in which ferricyanide is the final electron acceptor (the reporter mediator). After incubation of cells with mediators, steady state voltammetry of the ferri/ferrocyanide redox couple allows quantitation of the amount of mediator reduced by the cells. The plateau current at 425 mV vs Ag/AgCl gives the analytical signal. The results show that five of the mediators interact with at least three different trans Plasma Membrane Electron Transport systems (tPMETs), and that four mediators cross the plasma membrane to interact with cytoplasmic and mitochondrial redox molecules. Four of the mediators inhibit electron transfer from *S. cerevisiae*. Catabolic inhibitors were used to locate the cellular source of electrons for three of the mediators.

Redox mediators are used in fundamental studies of cell redox activity, for example, probing metabolic pathways and in applications such as cell biosensors and microbial fuel cells. Hydrophilic or lipophilic mediators can be used to access the major catabolic redox molecules of prokaryote cells because the redox centres are located in the cell membrane and are accessible extracellularly. In contrast, eukaryote cells have most of the catabolic redox sites located in the cytoplasm and mitochondria; these can only be accessed using a lipophilic mediator that can cross the cell membrane. Like all cells, however, eukaryotes have trans Plasma Membrane Electron Transport (tPMET) systems (also known as the plasma membrane oxido-reductase (PMOR) systems), which are accessible from the periplasm and can interact with hydrophilic mediators.

Electrochemical mediators can accept electrons from a eukaryote cell via a number of pathways. A hydrophilic mediator cannot cross the cell membrane and is restricted to interacting with tPMETs from the periplasm (Figure 1, pathway 1). An example is ferricyanide ($[Fe(CN)_6]^{3-}$), which is reduced to ferrocyanide ($[Fe(CN)_6]^{4-}$) by a ferri-reductase tPMET system that is embedded in the plasma membrane of *Saccharomyces cerevisiae*[1] and Merker et al. have shown that the reduction of toluidine blue O polyacrylamide (TBOP), a hydrophilic mediator, parallels the oxidation of cytoplasmic NADH[2]. A double mediator system (Figure 1, pathway 2) comprising lipophilic and hydrophilic mediators enables intracellular redox systems to be accessed. Lipophilic mediators can cross the cell membrane and interact with intracellular redox centres, become reduced and diffuse or are transported out of the cell to transfer electrons to a hydrophilic reporter mediator. In practice, lipophilic mediators usually cannot be used as the sole mediator because low aqueous solubility limits the mediator concentration and hence the magnitude of the signal. Additionally, often their limited stability in one redox state limits the techniques that can be used to probe the system. Double mediator systems using lipophilic menadione (MD) or 2,3,5,6-tetramethylphenylenediamine (2,3,5,6-TMPD), in conjunction with $[Fe(CN)_6]^{3-}$ have been used to investigate Chinese hamster ovary cells (CHO)[3] and *S. cerevisiae*[3–5]. The large signals observed in these studies could only have originated from intracellular redox molecules including those in the mitochondria. There are two other mechanisms by which a lipophilic mediator could transfer electrons to a reporter mediator. In the first, the reduced lipophilic mediator interacts with intracellular tPMET sites, which then passes the electron across the membrane to reduce the reporter mediator (Figure 1,

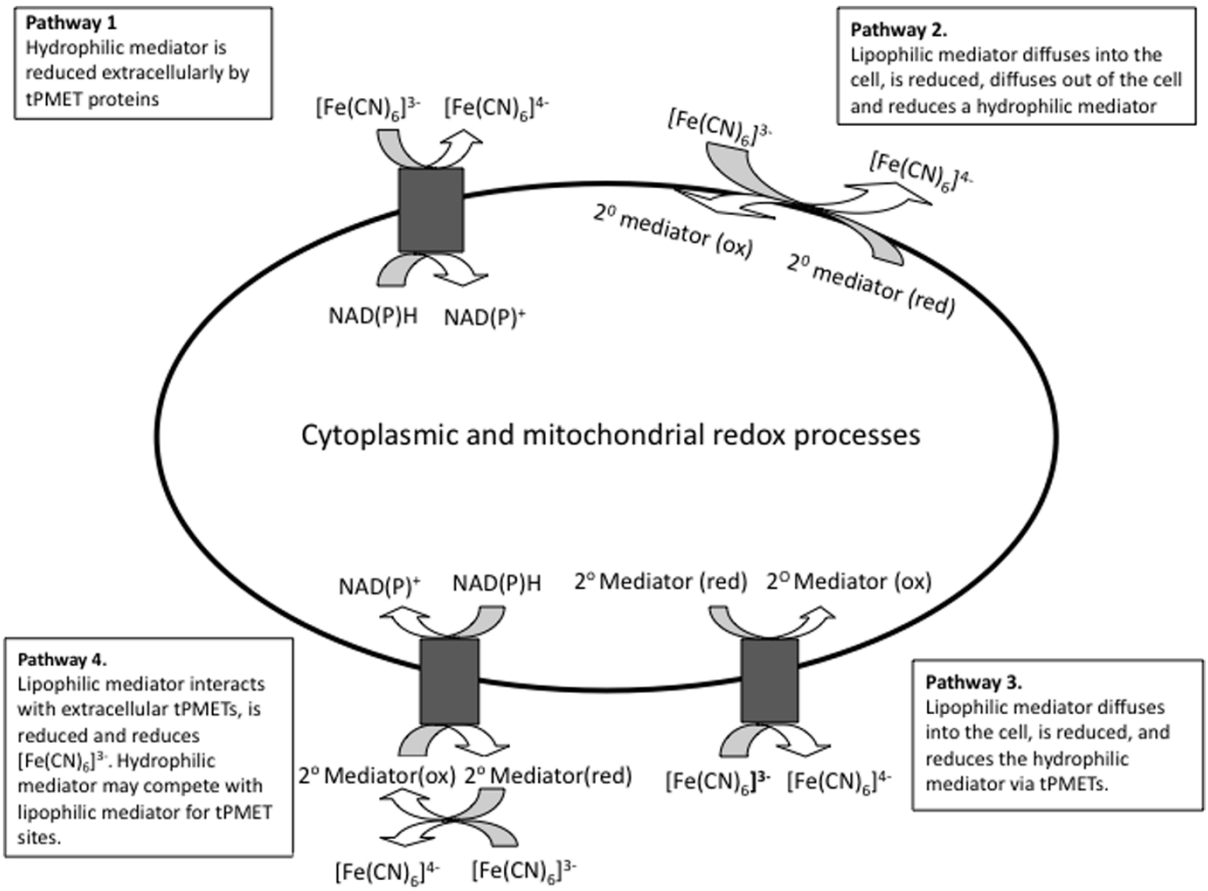

Figure 1 | Diagrammatic representation of the possible mechanisms by which a hydrophilic reporter mediator ($[Fe(CN)_6]^{3-}$) and a secondary mediator can interact with eukaryote cells and with each other. ■ = tPMET proteins.

pathway 3). This will only occur if the potential of the mediator is lower than the internal site of the tPMET. In the second mechanism (Figure 1, pathway 4), the mediator is reduced extracellularly by a tPMET system that then transfers its electrons to the reporter mediator[6]. Note: the signal size from pathway 4 will be very small relative to signals from pathway 2 because pathway 4 is only accessing tPMETs whereas in pathway 2, the mediator accesses intracellular redox molecules. It is likely that more than one of these pathways is operating simultaneously in any double mediator system investigation.

The aim of this investigation is to understand the interaction of *S. cerevisiae* with thirteen mediators that are commonly used to probe bacterial cell redox behaviour[7]. Although structurally different, yeast have essentially the same redox processes as bacteria and providing the mediators can access the redox site, it could be expected that the mediators would behave as they do with bacterial redox sites. Hydrophilic ferricyanide ($[Fe(CN)_6]^{3-}$) is used to report the interactions of the mediators with cell redox sites because it has stable Fe(II) and Fe(III) redox states, has well-behaved electrochemistry and has a formal electrode potential that is high enough to oxidise the reduced forms of all of the trial mediators. $[Fe(CN)_6]^{3-}$ is known not to cross the cell membrane, that is, it remains extracellular and is only reduced to a small extent by tPMET sites[4] and possibly by electrons transported across the cell wall[8]. Furthermore, previous double mediator studies using $[Fe(CN)_6]^{3-}$ with MD and 2,3,5,6-TMPD[3–5] suggest that there are no kinetic limitations on electron transfer between $[Fe(CN)_6]^{3-}$ and the lipophilic mediator, even though these mediators undergo two electron, proton-coupled transfers. It is possible to further investigate both the function of catabolic pathways and the interaction sites of mediators by using mediators in conjunction with agents that block pathways at specific sites[3,9]. In this study, two inhibitors, dicumarol and 6-aminonicotinamide (6-AN) are used. They were selected because each is known to target different sections of the cell redox systems and also were expected to be useful in further elucidating the interaction of mediators with intracellular and tPMET redox sites.

This study has quantified the relative efficiency of electron capture by each mediator, provided insight into the site of electron capture and for some mediators revealed an inhibitory effect.

Results and Discussion

Electrochemical detection of catabolism using steady-state voltammetry. Steady-state voltammetry is a convenient method for determining the amounts of oxidised and reduced forms of an electroactive species in solution. The position of the voltammogram on the current axis gives an immediate indication of the proportions of each oxidation state, and the anodic and cathodic plateau currents allow quantitation of each redox form. The linear sweep voltammogram (LSV) of $[Fe(CN)_6]^{3-}$ (Figure 2 scan A) shows only cathodic current, which arises from the reduction of $[Fe(CN)_6]^{3-}$ to $[Fe(CN)_6]^{4-}$. The absence of anodic current indicates, as expected, that there is no $[Fe(CN)_6]^{4-}$ in the bulk solution. When $[Fe(CN)_6]^{3-}$ was incubated with cells, a relatively small proportion of the $[Fe(CN)_6]^{3-}$ was reduced to $[Fe(CN)_6]^{4-}$ as evidenced by the small anodic current at potentials positive of 0.3 V (Fig. 2 scan B). $[Fe(CN)_6]^{3-}$ is hydrophilic and can only interact with redox sites that are embedded in the cell membrane and exposed to the periplasm. These tPMETs only transfer a small proportion of cellular electrons to the periplasm resulting in the relatively small signal. After incubation for 1 h with cells, glucose, $[Fe(CN)_6]^{3-}$ and the

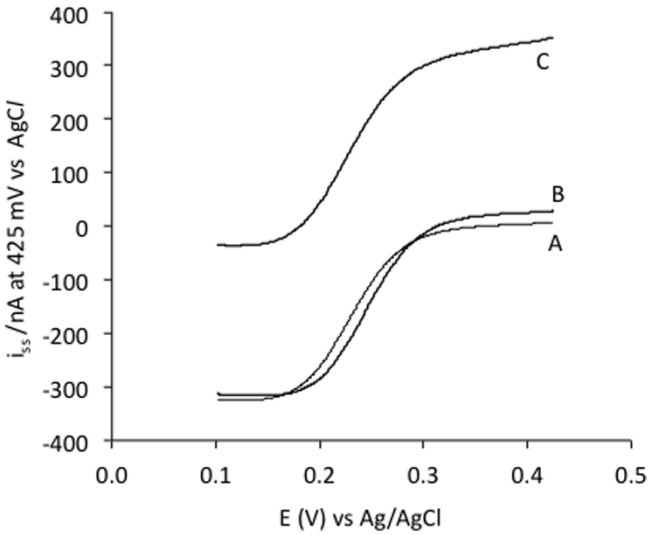

Figure 2 | Typical linear sweep voltammograms obtained for solutions of 20 mM $[Fe(CN)_6]^{3-}$ in the absence (A) and presence (B) of *S. cerevisiae.* Scan (C) was obtained from a solution containing cells, $[Fe(CN)_6]^{3-}$ (20 mM) and MD (100 μM). Standard incubation conditions were used.

lipophilic mediator, MD, the voltammogram (Fig. 2 scan C) has shifted up the current axis and there is mainly anodic current which arises from the oxidation of $[Fe(CN)_6]^{4-}$ and a small cathodic current which arises from reduction of unreacted $[Fe(CN)_6]^{3-}$. The large amount of reduced mediator is attributed to the lipophilicity of MD which allows it to cross the cell membrane, enter the cell and accept electrons from a large number of redox molecules[3]. MD, in the reduced form, returns to the extracellular environment and transfers its electrons to $[Fe(CN)_6]^{3-}$ generating $[Fe(CN)_6]^{4-}$, which is oxidised at the electrode.

The steady-state anodic plateau current measured at E = 425 mV was used as a relative measure of the amount of $[Fe(CN)_6]^{4-}$ produced, and hence the sum of yeast catabolism. Although the current at E = 425 mV can be measured without recording the full voltammogram, the full voltammogram provides a check of the reliability of the measurement, because any problems such as reduced sensitivity due to electrode fouling are easily detected. At the concentrations used in this work, none of the secondary mediators gave electrochemical responses that interfered with that of $[Fe(CN)_6]^{3-}$.

Assays with secondary mediators. The interactions of the thirteen trial or 'secondary' mediators with cells were quantified by performing double mediator experiments with $[Fe(CN)_6]^{3-}$ as the reporter mediator. Cells, trial mediator and reporter mediator were incubated for 1 h as described above. Incubations without cells i.e. acellular controls were also performed for each double mediator combination. At the end of incubation, solution pH was measured, cells, if present, were removed by centrifugation and the supernatants were analysed using steady-state LSV. The voltammograms produced were similar to those shown in Figure 2. The steady state anodic currents were measured at 425 mV, giving the relative amounts of $[Fe(CN)_6]^{3-}$ converted to $[Fe(CN)_6]^{4-}$ in each experiment. Figure 3 shows the mean steady state anodic currents for the thirteen secondary mediators and the controls. The currents were blank-corrected by subtracting the mean steady state anodic currents of the acellular trials. For the single mediator system i.e. $[Fe(CN)_6]^{3-}$ only, the anodic currents for $[Fe(CN)_6]^{4-}$ with and without cells are the mean of eleven replicates (33 measurements). An ANOVA shows that there is a significant difference between the with-cells and without-cells trials ($p < 0.00001$). In the double mediator systems, the amount of $[Fe(CN)_6]^{3-}$ converted to $[Fe(CN)_6]^{4-}$ varies widely.

Table 1 lists the redox potentials (versus SHE) of the mediators, the mean steady-state anodic currents at 425 mV, and the octanol partition coefficient (log P) of each secondary mediator, (for *N,N,N′N′*-TMPD, the hexane partition coefficient is given)[10]. Also tabulated is the number of electrons transferred in redox reactions of the mediators at pH 7.

Cells were cultivated with glucose at a concentration that will induce catabolite repression, i.e. mitochondrial RNA synthesis will be repressed and the cell will use the fermentation pathway to generate ATP. Repression can be reversed and respiration resumed if the repressing substrate is removed and a non-repressing substrate such as glycerol or ethanol is provided[11]. In these trials respiration can only occur if the mitochondria can be de-repressed by the mediator. Zhao et al. showed that menadione can restore respiration to glucose-repressed *S. cerevisiae* in anaerobic conditions[5] and De Santis et al. have shown that 2,3,5,6,-TMPD, and *N,N,N′N′*-TMPD can restore respiration to a ubiquinone-deficient nuclear mutant of *S. cerevisiae* by enabling electron transport[12]. It has also been shown that respiration could be restored in the rat liver mitochondrial electron transport chain that was blocked by rotenone by adding menadione. It was proposed that menadione was able to bypass the rotenone block at the complex I/ubiquinone interface and feed electrons back into the respiratory chain to allow the synthesis of ATP[13]. In addition Fain has shown that both menadione and vitamin K_5 increased respiration, glucose oxidation, lactate accumulation, and fatty acid synthesis[14].

The results of the double mediator experiments (Figure 3) place the mediators in three groups. In the first group, anodic steady state currents higher than the $[Fe(CN)_6]^{3-}$ cell control were obtained for safranine, benzoquinone, gallocyanine, DCIP, MD, methyl red, 2,3,5,6-TMPD and *N,N,N′,N′*-TMPD, indicating that all these molecules have access to redox sites that $[Fe(CN)_6]^{3-}$ cannot access. The second group, 1-M-PMS and resorufin, have signals the same size as the $[Fe(CN)_6]^{3-}$ cell control, and the third group of neutral red, phenazine ethosulphate and toluidine blue, have signals lower than the $[Fe(CN)_6]^{3-}$ cell control.

Considering the latter group first, it is likely that these molecules are inhibitory to the cells possibly causing metabolic disruption or loss of cell membrane integrity. Neutral red is known to cross the cell membrane, for example it is used to distinguish viable yeast cells from dead cells[15]. In higher organisms neutral red is sequestered by the lysosomes[16], which is an analogue of the yeast vacuole[17], and thus probably could not be involved in electron transfer. Phenazine ethosulphate toxicity may be due to the high yield of the pyridine nucleotide radical, 5-hydroxy-5,5-dimethylpyrrolidino-1-oxyl (DMPO-OH), which is formed largely from the interaction of phenazine ethosulphate and NADH which results in a decrease in the NAD^+/NADH pool[18]. This result is, however, different from the findings of Pasco et al.[19] who report that phenazine ethosulphate increased $[Fe(CN)_6]^{3-}$ reduction in a bacterium. In the case of toluidine blue, Ito reported that the yeast cell wall prevents the molecule accessing the cytoplasmic membrane of the cell, however he also noted that toluidine blue can be photoactivated to become toxic to cells[20].

The conversion of $[Fe(CN)_6]^{3-}$ to $[Fe(CN)_6]^{4-}$ in the presence of 1-M-PMS and resorufin is not significantly different from the $[Fe(CN)_6]^{3-}$ cellular control. Tan et al.[6] suggest that 1-M-PMS interacts with the same tPMET sites as $[Fe(CN)_6]^{3-}$. Our result supports this proposal because, if 1-M-PMS (and resorufin) competes with $[Fe(CN)_6]^{3-}$ for the same tPMET electrons, $[Fe(CN)_6]^{3-}$ will oxidise any reduced 1-M-PMS or resorufin resulting in a signal that is of the same magnitude as the $[Fe(CN)_6]^{3-}$ control signal. Figure 4A shows that there is not a strong correlation between signal size and log P. For example log P of MD is less than that of methyl red, yet the MD current is almost 9 times larger than the methyl red current. Considering the benzoquinone, safranine, gallocyanine and methyl red group, methyl red is an azo dye and Ramalho et al. have shown

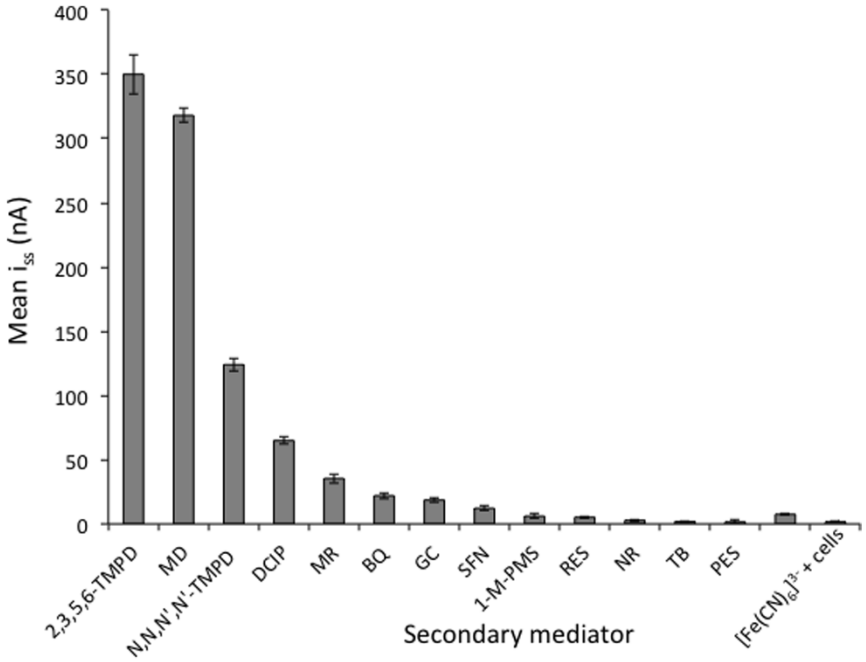

Figure 3 | Plot of mean steady state currents measured from linear sweep voltammograms at 425 mV vs Ag/AgCl obtained for solutions of 20 mM $[Fe(CN)_6]^{3-}$ and 100 μM secondary mediator, using standard incubation and assay conditions. Each current has been corrected with the acellular control values; error bars represent ±1SE (n = 9 except for $[Fe(CN)_6]^{3-}$ + cells and $[Fe(CN)_6]^{3-}$ controls, n = 33).

that the ferri-reductase tPMET system of *S. cerevisiae* is involved in the extracellular reduction of azo dyes. The study found that deletion of the FRE 1 gene encoding the tPMET protein does not completely remove azo activity and hence the reduction is probably not totally dependent on tPMETs[21]. Jahdav et al.[22] also report that reduction of methyl red remains extracellular in *S. cerevisiae*. There is one report on the use of safranine as a tool for investigating variations in membrane potential by fluorescence microscopy however in that study, the cells were first permeabilised with digitonin[23]. We have not found relevant information on the redox interaction of benzoquinone and gallocyanine with eukaryote cells. Nevertheless, the currents for these mediators are significantly greater than for $[Fe(CN)_6]^{3-}$ alone, indicating that they probably interact with tPMET sites not accessible to $[Fe(CN)_6]^{3-}$, 1-M-PMS and resofurin. For methyl red, benzoquinone, gallocyanine and safranine, the anodic current increases as the formal potential increases (Table 1). Figure 5A shows a plot of the log of the mean steady-state current versus the potential of these (and other) mediators. A linear relationship between these parameters is expected if the rate of reduction of the secondary mediator is controlled by the difference in potential between the formal potentials of the mediator and the cellular redox site(s), that is, the thermodynamic driving force. A R^2 value of 0.895 is obtained for a linear fit to the data for methyl red, benzoquinone, gallocyanine and safranine, however with the removal of the benzoquinone datum point, the R^2 value becomes 0.985 (Figure 5A, inset). This analysis is consistent with interaction of gallocyanine, methyl red and safranine with the same tPMET site or with different tPMET sites with the same redox potential, whereas benzoquinone interacts with a tPMET site that has a different redox potential. Considering the data in a different way and assuming that electron transfer from cellular redox

Table 1 | Standard redox potential of mediators (E^o) versus SHE[7] and the mean magnitude of the steady state oxidation current (i_{ss}) obtained from LSVs at 425 mV vs Ag/AgCl of double mediator solutions incubated with cells. Log P values for NR SFN, GC, MD, DCIP, BQ, MR are for octanol/water. The log P value for *N,N,N′,N′*-TMPD is for hexane/water. ^Log P values were calculated using ChemDraw (http://www.cambridgesoft.com)

Mediator	E^o (V)	Mean i_{ss}/nA ± 1SE.	Log P	Electrons transfered
NR	−0.325	2.8 ± 0.9	−0.95 [41]	$1e^-$
SFN	−0.289	12.2 ± 1.9	0.4 [42]	$2e^-$
TB	−0.027	1.9 ± 0.4	−0.9 [42]	$2e^-$
GC	0.03	18.6 ± 1.6	1.56 [43]	$2e^-$
MD	0.03	318 ± 5	1.58 [44]	$2e^-$
PES	0.055,	1.5 ± 1.5	3.06^	$2e^-$
RES	0.065	5.2 ± 0.9	1.77^	$2e^-$
1-M-PMS	0.08	6.1 ± 2.0	2.9^	$2e^-$
DCIP	0.217	64.9 ± 2.6	3.12 [47]	$2e^-$
***N,N,N′,N′*-TMPD**	0.25	124 ± 5	5.6 [10]	$1e^-$ *
2,3,5,6-TMPD	0.257	350 ± 15	2.37^	$2e^-$
BQ	0.28	22.0 ± 2.3	0.18 [45]	$2e^-$
MR	0.37	35.4 ± 3.6	1.67 [46]	$2e^-$
$[Fe(CN)_6]^{3-}$	0.46	7.5 ± 0.3	−0.26^	$1e^-$

*N,N,N′,N′-TMPD is a 2 electron transfer process but in this application it acts as a 1 electron transfer reduction because the second reduction step is irreversible[18].

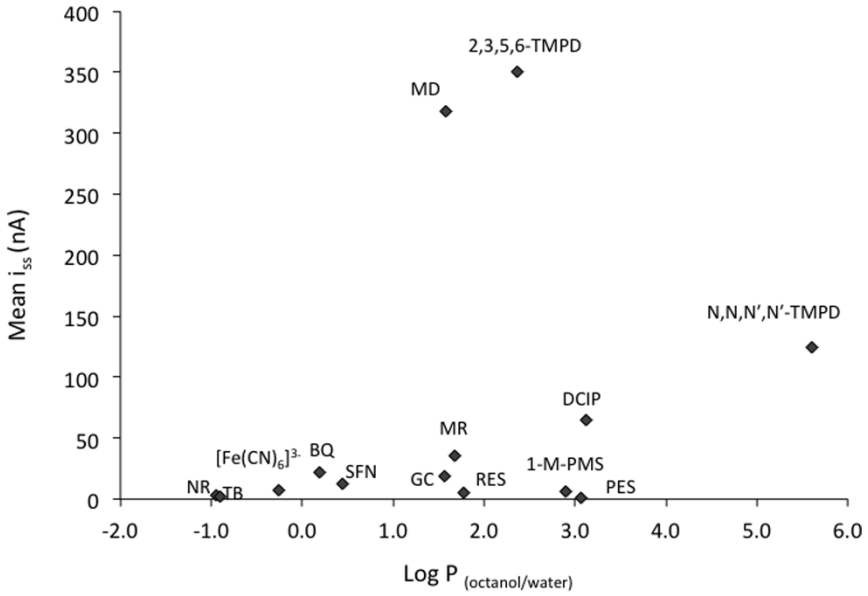

Figure 4 | Plot of mean steady state currents (i_{ss}) obtained from linear sweep voltammograms at 425 mV vs Ag/AgCl versus concentration partition coefficients (log P) for BQ, SFN, GC, MD, DCIP, MR, and *N,N,N′,N′*-TMPD.

sites to the secondary mediator is fast and not rate-limited, the mean current should depend on the number of tPMET sites, which are thermodynamically able to reduce the mediator. Figure 5B shows a plot of mean current generated versus formal potential of the mediators. This plot suggests that methyl red, benzoquinone, gallocyanine and safranine may interact with additional tPMET sites to that accessible to Fe^{III}, 1-M-PMS and resofurin. Methyl red accepts electrons from three additional tPMET sites, benzoquinone and gallocyanine from two and safranine from one. Both of the analyses outlined above support the notion that these mediators are interacting externally with at least two tPMET sites additional to that accessible to Fe^{III}, 1-M-PMS and resofurin (Figure 1, pathway 4). We tentatively propose that the resofurin, PMS and $[Fe(CN)_6]^{3-}$ signals are not related to their redox potentials because these mediators may be interacting with non-voltage gated tPMETs, whereas the other mediators are interacting with voltage gated tPMETs.

2,3,5,6-TMPD, *N,N,N′,N′*-TMPD, MD and DCIP are known to cross the cell membrane and interact with cell redox sites[4,5,11,24,25]. Figure 4B shows that log P (lipophilicity) and standard redox potential are not correlated with the signal size, for example MD is less lipophilic than DCIP and *N,N,N′,N′*-TMPD but generates a significantly larger signal. Similarly the data in Table 1 show that the signal size is not directly related to the redox potential of the mediator. Signal size also does not appear to be related to methods of transport of the mediator into and out of the cell, e.g. MD and 2,3,5,6-TMPD give signals of very similar sizes but their modes of transport are different. MD and its oxidation product menadiol are neutral and can diffuse across the cell membrane[25] while the redox active menadione conjugate, menadione-S-glutathione (thiodine), is actively transported out of the cell[25,26]. 2,3,5,6-TMPD on the other hand, is a charged molecule and must be actively transported into the cell. 2,3,5,6-TMPD voltammetry shows a reversible 2 electron exchange and it is expected to function as a two-electron mediator[27]. The signal from *N,N,N′,N′*-TMPD is however, less than half the size of that from 2,3,5,6-TMPD, which may be in part because it acts as a one-electron transfer mediator[28].

The pH of the incubation medium at the end of incubation varied (Table 1), with the mediators that gave the largest signals (2,3,5,6-TMPD, *N,N,N′,N′*-TMPD and MD) resulting in a significant pH decrease. This may simply reflect the level of cell activity, for example organic acid production, or the production of CO_2 from the Kreb

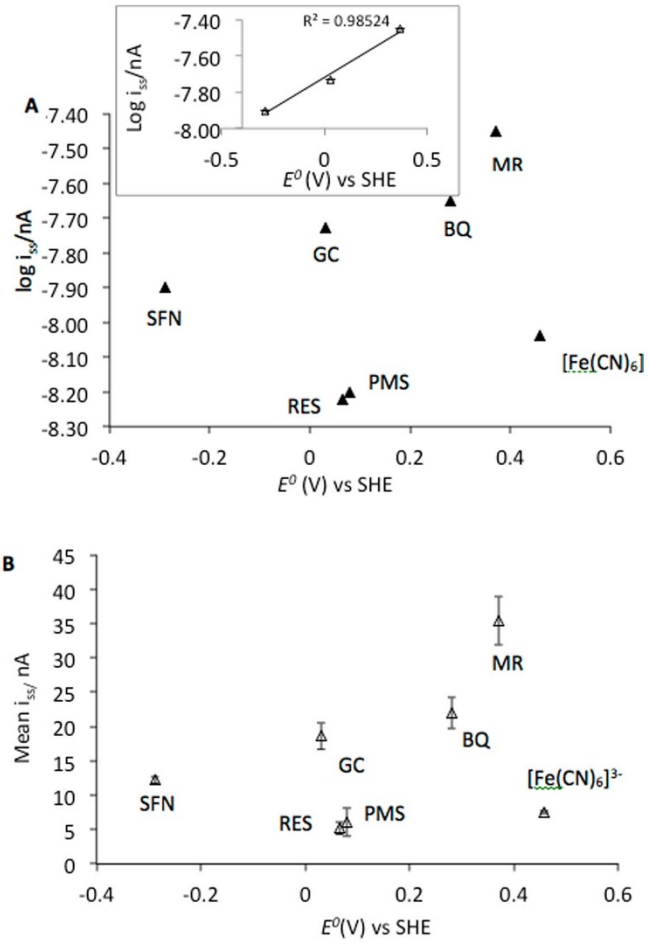

Figure 5 | (A) Plots of the log of the mean steady state currents at 425 mV vs Ag/AgCl versus the formal redox potential of each mediator. Inset graph shows the linearity of the relationship between SFN, GC and MR when BQ is removed from the plot. (B) Plot of the mean steady state currents at 425 mV vs Ag/AgCl against the formal redox potential versus SHE of the secondary mediators. Data obtained from Figure 3.

cycle. The expulsion of protons from the cell during active transport could also contribute to the decrease in pH. While this could be the case for both TMPD derivatives, MD, as noted above, is reported to passively diffuse into the cell[25], that is, without the expulsion of protons. pH affects the $E_{1/2}$ of redox molecules that transfer electrons and protons i.e. pH dependent mediators. Intracellular pH is controlled at pH 7.2 in the presence of glucose and remains relatively constant when the external pH is in the range of 3–7.5[29]. The extracellular pH did not decrease below pH 3.3 in any of the trials and hence the intracellular mediator interactions would occur at ~pH 7.2. Considering the effect of pH on the reaction between $[Fe(CN)_6]^{3-}$ and secondary mediators outside the cell, the decrease in pH seen during the incubation period makes the electron transfer between reduced pH-dependent secondary mediators (MD, *N*,*N*,*N*′,*N*′-TMPD and 2,3,5,6- TMPD) and $[Fe(CN)_6]^{3-}$ thermodynamically less favourable than at pH 7. However, the size of these signals, make any thermodynamic restriction irrelevant in the context of these experiments.

We conclude that the differences in signal sizes for those mediators that act intracellularly with *S. cerevisiae* are primarily determined by their ability to interact with internal redox sites. Other workers have drawn similar conclusions. For example, Zhao et al.[5] showed that in anaerobic trials with S. *cerevisiae* using a double mediator system, signals from *N*,*N*,*N*′,*N*′-TMPD were about one fifth of the size of signals obtained with MD. Analysis of the growth media showed that ethanol production with MD was only 14% of the theoretical possible while it was 73% with *N*,*N*,*N*′,*N*′-TMPD. They proposed that MD acts as a terminal electron acceptor in the electron transport chain so that respiration proceeds in anaerobic conditions, resulting in a larger electrochemical signal and lower ethanol production whereas *N*,*N*,*N*′,*N*′-TMPD predominately interacts with fermentation resulting in higher ethanol production and a smaller signal.

However redox potential, lipohilicity and mode of transport of the mediator are likely to have some influence. A similar conclusion was reached by Lui et al.[25], who concluded that in general the main factors limiting the overall charge transfer rate in scanning electrochemical microscope (SECM) experiments with mammalian cells can be either membrane transport, the availability of intracellular redox agents, or the driving force for the redox reaction. Although Tatsumi *et al.* found that the rate-limiting step in the catabolism of a substrate was diffusion in the external medium, the extracellular medium in our experiments was stirred by nitrogen sparging thus removing the rate limitation imposed by diffusion of mediators[30].

Double mediator experiments in the presence of cellular inhibitors. The metabolism inhibitors, dicumarol and 6-AN, were used to provide further evidence on the interaction of the mediators with redox sites. Dicumarol affects respiration in a number of ways both increasing and decreasing enzymes involved in these pathways[31]. Selection of 6-AN was based on its inhibition of 6-phosphogluconate dehydrogenase in the Pentose Phosphate Pathway (PPP), which results in a decrease in NADPH production[32]. The secondary mediators DCIP and gallocyanine were selected for this study because their interactions with the cell were expected to be straightforward. DCIP is a mediator that has been reported to interact with a limited number of internal redox sites e.g. it has been reported to preferentially interact with the fermentative pathway[33] and interacts with respiratory processes only in the presence of inhibitors[34]. Gallocyanine is an example of a mediator that gives a small response in the double mediator system and has not been reported to interact intracellularly. On the other hand, MD and 2,3,5,6,-TMPD are known to interact with a wide range of cell redox molecules including those in the mitochondria and hence would be expected to give data that was difficult to interpret[35]. Controls containing $[Fe(CN)_6]^{3-}$ and the metabolism inhibitors were also performed. Measurement of the conversion of $[Fe(CN)_6]^{3-}$ to $[Fe(CN)_6]^{4-}$ for each mediator/inhibitor combination is shown in Figure 6A ($[Fe(CN)_6]^{3-}$ only), 6B ($[Fe(CN)_6]^{3-}$ and DCIP) and 6C ($[Fe(CN)_6]^{3-}$ and gallocyanine). The patterns of responses of each system to the inhibitors were compared to determine the sites of interactions and two-way ANOVAs and a post-hoc Tukey test were used to verify differences or similarities of the signals within and between each group.

When cells were incubated with inhibitors and $[Fe(CN)_6]^{3-}$ only (Figure 6A), the mean oxidation currents showed that there were significant differences between assays with no inhibitors and with each of the single inhibitors, but not with assays containing both inhibitors. The oxidation signal with dicumarol was over two times greater ($p < 0.05$) than when the dicumarol was absent. $[Fe(CN)_6]^{3-}$ is reduced by both NADPH and NADH dependent ferri-reductases (tPMETs)[36,37] and the observed increase occurs because, when dicumarol uncouples NADH-cytochrome-b5 in the mitochondria[38], PPP activity rises in an attempt to provide the cell with energy[39]. This results in an increase in NADPH, which, is subsequently oxidised by a membrane-bound ferri-reductase to ensure the pool of $NADP^+$ is not depleted[37]. The mean currents obtained for $[Fe(CN)_6]^{3-}$ reduction in the presence of 6-AN are also significantly higher than in its absence ($p < 0.00001$). Inhibition of PPP by 6-AN should lead to a decrease in the signal and hence the increase suggests that an unknown pathway of NADPH production increases in activity to compensate for the decrease in the activity of the PPP; this finding is in agreement with Davis and Kauffmann[32]. Further evidence for the existence of another NADPH synthesising pathway can be seen when both inhibitors are present. The signal is significantly lower than the signals obtained when single inhibitors are used, but it is the same as that in the absence of inhibitors ($p < 0.001$). With dicumarol depressing the concentration of NADH and 6-AN depressing PPP and the production of NADPH, the signal should fall significantly. The fact that the signal is the same as the control also supports the notion of another NADPH synthesis pathway.

DCIP is known to interact with internal cell redox sites. When cells were incubated with $[Fe(CN)_6]^{3-}$ and DCIP (Figure 6B), the mean oxidation currents were significantly different for assays with no inhibitors, with dicumarol, with 6-AN, and for assays containing both of these inhibitors ($p < 0.0001$). The current increased approximately 50% ($p < 0.0001$) when dicumarol was added to assays with DCIP and $[Fe(CN)_6]^{3-}$. This is probably because dicumarol inhibits complex II, III and IV of the electron transport chain[31] resulting in the concentration of reduced DCIP increasing because the cell can no longer transfer its electrons to cytochrome b, i.e. the cell uses DCIP as a terminal redox molecule in an attempt to allow the electron transport chain to continue. Additionally dicumarol induces a strong uncoupling effect on the electron transport chain[38], which increases oxidation currents when DCIP is present, i.e. there is an increase in DCIP reduction in the mitochondria in an attempt to restore the transmembrane proton gradient to allow ATP production to continue. This suggests that DCIP interacts with redox molecules in the mitochondria, which is in agreement with the findings of Kumar and Acharya[34], but is contrary to the findings of Zhao et al[5]. In the presence of 6-AN, the signal obtained for DCIP is higher than when the assay was performed in the absence of 6-AN. It has been shown that this inhibitor depresses PPP and lowers the production of NADPH[40]. The reason for the unexpected increase in current is unclear at present and requires further investigation. It may indicate that either mitochondrial metabolism is disrupted and, as seen with dicumarol, DCIP is used to maintain electron transport and/or, as suggested earlier, there is another pathway for NADPH production.

When cells were incubated with $[Fe(CN)_6]^{3-}$ and gallocyanine without inhibitors, with dicumarol, with 6-AN and with both inhibitors (Figure 6C), there were no significant differences between the signals ($p > 0.9$). Comparison of the trials using $[Fe(CN)_6]^{3-}$ as the

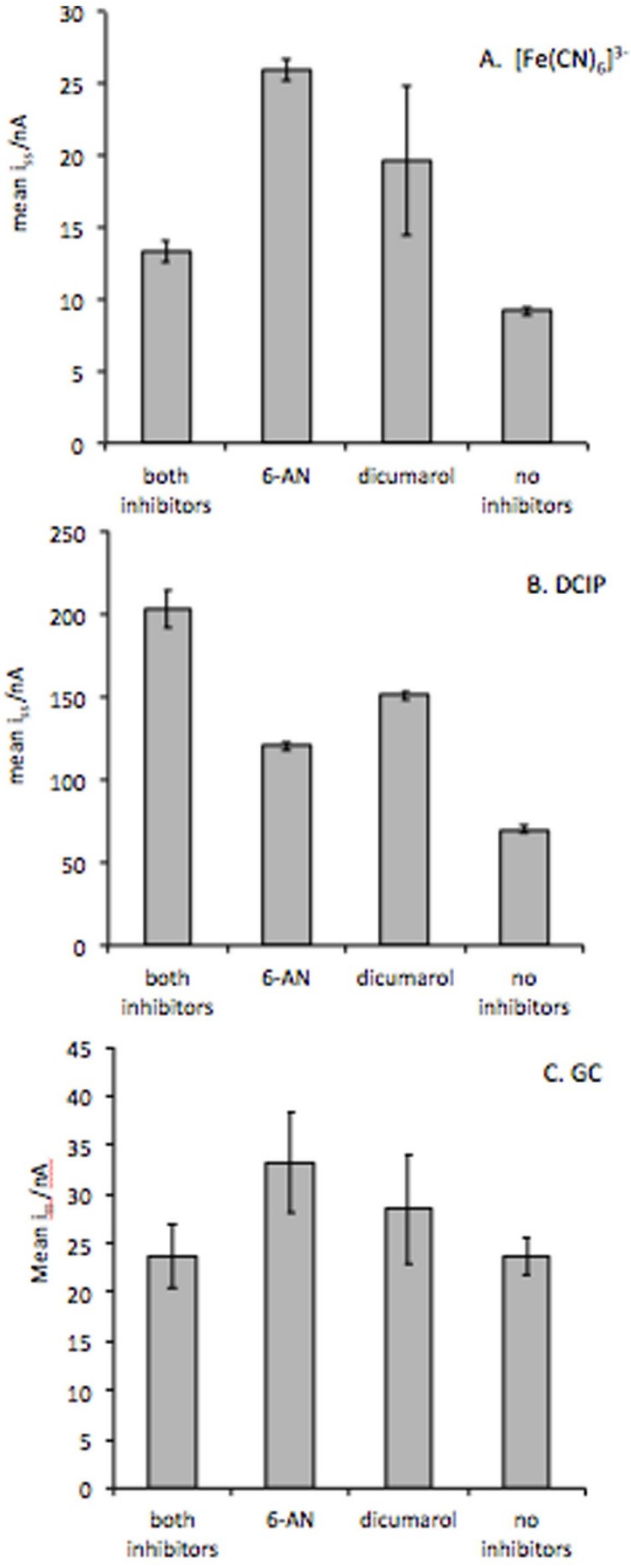

Figure 6 | Mean steady state currents from LSVs of cells incubated with solutions of: 20 mM $[Fe(CN)_6]^{3-}$ only (A); Mean steady state currents from LSVs of cells incubated with solutions of 20 mM $[Fe(CN)_6]^{3-}$ and 100 μM DCIP (B); and Mean steady state currents from LSVs of cells incubated with solutions of 20 mM $[Fe(CN)_6]^{3-}$ and 100 μM GC (C) at 425 mV vs Ag/AgCl. Each group was incubated with no inhibitors, dicumarol (100 μM), 6-AN (100 μM), and both inhibitors. Standard incubation conditions were used. Error bars represent ±1SE (n = 9).

only mediator (Figure 6A), and the trials using $[Fe(CN)_6]^{3-}$ and gallocyanine (Figure 6C), shows that while there is no significant difference between each of the inhibitor groups (dicumarol, 6-AN and both inhibitors), there is a significant difference between the 'no inhibitors' response in each trial (Figure 6A and 6C). This confirms that gallocyanine is receiving electrons from surface sites additional to those accessed by $[Fe(CN)_6]^{3-}$. In the presence of inhibitors however, the gallocyanine system is indistinguishable from the $[Fe(CN)_6]^{3-}$ only system, suggesting that the inhibitors act on redox processes within the cell to significantly decrease the supply of electrons to the surface site(s) that gallocyanine interacts with, while increasing the supply of electrons to tPMETs that $[Fe(CN)_6]^{3-}$ interacts with.

Conclusion

This study shows that the use of a hydrophilic reporter mediator with a high formal redox potential is an effective strategy to study the interactions of other mediators with eukaryote cell redox processes. The method distinguishes mediators that interact only with transmembrane electron transport molecules from those that interact with intracellular redox sites. The addition of blocking agents to the cells allows further differentiation between different types of tPMET site and differentiation between the different intracellular redox sites such as glycolysis, the hexose monophosphate pathway and those of the mitochondria. In addition the method elucidates the redox interactions occurring in eukaryote cells in vivo. This work suggests that $[Fe(CN)_6]^{3-}$, resofurin, 1-M-PMS, safranine, gallocyanine, benzoquinone and methyl red interact with several tPMET sites on the external surface of the cell membrane i.e. extracellularly. $[Fe(CN)_6]^{3-}$, resofurin and 1-M-PMS may interact with a non-voltage gated tPMET while gallocyanine appears to interact with a tPMET which functions independently of NADH/NADPH. The responses of the lipophilic mediators, 2,3,5,6-TMPD, MD, *N,N,N′,N′*-TMPD and DCIP, which interact intracellularly, however do not have a simple relationship with mediator redox potentials, lipophilicity or mode of transport into and out of cells.

Methods

Cell culture. *S. cerevisiae* (NTC 10716) was maintained on YEPD agar at 4°C. Yeast cultures were grown in 150 ml of YEPD broth in shake flasks rotated at 180 rpm for 16 h at 30°C. Cells were then harvested by centrifugation at 4500 × g and washed twice in 25 ml of 50 mM phosphate buffer pH 7 before being re-suspended in sterile phosphate buffered saline (PBS, 50 mM K_2HPO_4/KH_2PO_4, pH 7, 100 mM KCl). The optical density of the cell suspension was adjusted to give an OD_{600} of 40 using an LKB Novaspec II spectrophotometer. Cells were used on the day of harvest.

Chemicals. Stock solutions of chemicals were prepared as follows. The reporter mediator, potassium hexacyanoferrate, (Sigma-Aldrich), was dissolved in sterile PBS to give a final concentration of 200 mM. The secondary mediators: benzoquinone, BQ, (Sigma), dichloroindophenol, DCIP, (Sigma), gallocyanine, GC, (Sigma), menadione, MD, (Sigma), 1-methoxy phenazine methosulphate, 1-M-PMS, (Dojindo Laboratories), methyl red, MR, (M&B), neutral red, NR, (Sigma), phenazine ethosulphate, PES, (Sigma), resorufin, RES, (Sigma), safranine, SFN, (BDH), *N,N,N′,N′*-tetramethylphenylenediamine, *N,N,N′,N′*-TMPD, (Sigma), 2,3,5,6-tetramethylphenyldiamine, TMPD, 2,3,5,6-TMPD (Sigma) and toluidine blue, TB, (BDH), were dissolved in 96% ethanol to give 2 mM solutions. Ethanol does not contribute to the signal because alcohol dehydrogenase 2 (ADH 2), which catalyses the conversion of ethanol to acetaldehyde, is completely repressed in the presence of a fermentable substrate. Glucose (Merck) was dissolved in sterile PBS to give a 7.5 mM solution. A 2 mM stock solution of dicumarol (Sigma) was prepared in distilled water with the addition of 1 M sodium hydroxide until the dicumarol had dissolved. 6-aminonicotinamide, 6-AN (Sigma) was dissolved in 96% ethanol to give a 2 mM solution.

Assay conditions

Double mediator system. Standard assay and incubation conditions were as follows: a total assay volume of 5 ml comprised 20 mM $[Fe(CN)_6]^{3-}$, 100 μM secondary mediator, 7.5 mM glucose and cells at OD_{600} of 5.0. Three controls were used; control 1 comprised 20 mM $[Fe(CN)_6]^{3-}$, 7.5 mM glucose and cells at OD_{600} 5.0 (total volume 5 mL), control 2 comprised 20 mM $[Fe(CN)_6]^{3-}$ and

7.5 mM glucose (total volume 5 mL), and control 3 comprised 7.5 mM glucose with cells at an OD_{600} of 5.0 (total volume 5 mL). Assay solutions were incubated for 1 h at 37°C and purged with O_2-free N_2. Purging not only eliminated O_2 but also served to keep the cells in suspension. All assays were performed in triplicate. On completion, solutions were centrifuged at 4500 × g for 8 min and the supernatants were decanted into 50 mL tubes for immediate electrochemical analysis.

Metabolism disruptor studies. Double mediator studies were performed as above, but with the addition of the metabolism disruptors, dicumarol and 6-aminonicotinamide, both at a final concentration of 100 μM.

Electroanalysis of supernatants. Electrochemical investigation of the supernatants was performed using linear sweep voltammetry (LSV) under steady-state conditions. A three electrode system comprising a 100 μm Pt microdisc working electrode, a Ag/AgCl (3 M KCl) reference electrode, and a Pt counter electrode controlled by an eDAQ potentiostat and eDAQ power lab 2/20 with eCHEM data acquisition software was used in all experiments. The Pt microdisc electrode was polished before each measurement with 0.05 μm alumina on Lecloth. The Pt microdisc was held at open circuit potential for 10 s prior to beginning each scan and LSVs were obtained by scanning from 450 mV to 100 mV at a scan rate of 10 mV s^{-1}. Steady state currents were measured at 425 mV and three repeat voltammograms were averaged to give the mean value; five replicates were obtained for the $[Fe(CN)_6]^{3-}$ and cells control. The mean current from each replicate was used to obtain an overall experimental mean and standard error. The experiments were performed over a number of days so the statistical data reflects cell batch variation.

1. Qin, Y., Liu, L. M., Li, C. H., Xu, S. & Chen, J. Accelerating glycolytic flux of Torulopsis glabrata CCTCC M202019 at high oxidoreduction potential created using potassium ferricyanide. *Biotechnol. Prog.* **26**, 1551–1557 (2010).
2. Merker, M. P., Bongard, R. D., Kettenhofen, N. J., Okamoto, Y. & Dawson, C. A. Intracellular redox status affects transplasma membrane electron transport in pulmonary arterial endothelial cells. *Am. J. Physiol. Lung Cell Mol. Physiol.* **282**, L36–L43 (2002).
3. Rabinowitz, J. D., Vacchino, J. F., Beeson, C. & McConnell, H. M. Potentiometric measurement of intracellular redox activity. *J. Am. Chem. Soc.* **120**, 2464–2473 (1998).
4. Baronian, K., Downard, A., Lowen, R. & Pasco, N. Detection of two distinct substrate-dependent catabolic responses in yeast cells using a mediated electrochemical method. *Appl. Microbiol. Biotechnol.* **60**, 108–113 (2002).
5. Zhao, J. *et al.* The different behaviors of three oxidative mediators in probing the redox activities of the yeast *Saccharomyces cerevisiae*. *Anal. Chim. Acta* **597**, 67–74 (2007).
6. Tan, A. S. & Berridge, M. V. Distinct trans-plasma membrane redox pathways reduce cell-impermeable dyes in HeLa cells. *Redox Rep.* **9**, 302–306, doi:doi:10.1179/135100004225006777 (2004).
7. Fultz, M. L. & Durst, R. A. Mediator compounds for the electrochemical study of biological redox systems: a compilation. *Anal. Chim. Acta* **140**, 1–18 (1982).
8. Rawson, F. J., Gross, A. J., Garrett, D. J., Downard, A. J. & Baronian, K. H. Mediated electrochemical detection of electron transfer from the outer surface of the cell wall of *Saccharomyces cerevisiae*. *Electrochem. Comm.* **15**, 85–87 (2012).
9. Zhao, J. *et al.* Electrochemical insights into the glucose metabolism pathways within *Saccharomyces cerevisiae*. *Anal. Lett.* **38**, 89–98 (2005).
10. Banks, C. E., Rees, N. V. & Compton, R. G. Sonoelectrochemistry in acoustically emulsified media. *J. Electroanal. Chem.* **535**, 41–47 (2002).
11. Ulery, T. L., Jang, S. H. & Jaehning, J. A. Glucose repression of yeast mitochondrial transcription: kinetics of derepression and role of nuclear genes. *Mol. Cell Biol.* **14**, 1160–1170 (1994).
12. De Santis, A., Bertoli, E., Di Gioia, A., Melandri, B. & Melandri, A. B. The reconstitution of oxidative phosphorylation in mitochondria isolated from a ubiquinone-deficient mutant of *Saccharomyces cerevisiae*. *Bioneng. Biomem.* **14**, 159–169 (1982).
13. Klöhn, P.-C. & Neumann, H.-G. Impairment of respiration and oxidative phosphorylation by redox cyclers 2-nitrosofluorene and menadione. *Chem-Biol. Interact.* **106**, 15–28 (1997).
14. Fain, J. N. Effects of menadione and vitamin K5 on glucose metabolism, respiration, lipolysis, cyclic 3′, 5′-adenylic acid accumulation, and adenyl cyclase in white fat cells. *Mol. Pharmacol.* **7**, 465–479 (1971).
15. Naka, W., Hanyaku, H., Tajima, S., Harada, T. & Nishikawa, T. Application of neutral red staining for evaluation of the viability of dermatophytes and Candida in human skin scales. *Med. Mycol.* **32**, 31–35 (1994).
16. Repetto, G., del Peso, A. & Zurita, J. L. Neutral red uptake assay for the estimation of cell viability/cytotoxicity. *Nano. Lett.* **3**, 1125–1131 (2008).
17. Li, S. C. & Kane, P. M. The yeast lysosome-like vacuole: endpoint and crossroads. *Biochem. Biophys. Acta* **1793**, 650–663 (2009).
18. Davis, G. & Thornalley, P. Free radical production from the aerobic oxidation of reduced pyridine nucleotides catalysed by phenazine derivatives. *Bioenergetics* **724**, 456–464 (1983).
19. Pasco, N., Hay, J., Scott, A. & Webber, J. Redox coupling to microbial respiration: an evaluation of secondary mediators as binary mixtures with ferricyanide. *Aus. J. Chem.* **58**, 288–293 (2005).
20. Ito, T. Toluidine blue: the mode of photodynamic action in yeast cells. *Photochem. Photobiol.* **25**, 47–53 (1977).
21. Ramalho, P. A. *et al.* Azo reductase activity of intact *Saccharomyces cerevisiae* cells is dependent on the Fre1p component of plasma membrane ferric reductase. *Appl. Environ. Microbiol.* **71**, 3882–3888 (2005).
22. Jadhav, J., Parshetti, G., Kalme, S. & Govindwar, S. Decolourization of azo dye methyl red by *Saccharomyces cerevisiae* MTCC 463. *Chemosphere* **68**, 394–400 (2007).
23. Pacelli, C. *et al.* Tight control of mitochondrial membrane potential by cytochrome c oxidase. *Mitochondrion* **11**, 334–341 (2011).
24. Zhao, J., Wang, M., Yang, Z. & Yang, Z. Measurement of inhibitory effects of furfural and furfural alcohol using coupled redox mediators. *Enzyme Microb. Technol.* **37**, 246–253 (2005).
25. Liu, B., Rotenberg, S. A. & Mirkin, M. V. Scanning electrochemical microscopy of living cells: Different redox activities of nonmetastatic and metastatic human breast cells. *Proc. Natl. Acad. Sci. USA* **97**, 9855–9860 (2000).
26. Mauzeroll, J. & Bard, A. J. Scanning electrochemical microscopy of menadione-glutathione conjugate export from yeast cells. *Proc. Natl. Acad. Sci. USA* **101**, 7862–7867, doi:10.1073/pnas.0402556101 (2004).
27. Long, J. S. *et al.* Oxidation of several p-phenylenediamines in room temperature ionic liquids: Estimation of transport and electrode kinetic parameters. *J. Phys. Chem. C* **112**, 6993–7000 (2008).
28. Maruthamuthu, P., Venkatasubramanian, L. & Dharmalingam, P. A fast kinetic study of the formation and decay of N, N, N′, N′-tetramethyl-p-phenylenediamine radical cation in aqueous solution. *J. Chem. Soc. Faraday Trans.* 1 **82**, 359–363 (1986).
29. Orij, R., Postmus, J., Ter Beek, A., Brul, S. & Smits, G. J. In vivo measurement of cytosolic and mitochondrial pH using a pH-sensitive GFP derivative in *Saccharomyces cerevisiae* reveals a relation between intracellular pH and growth. *Microbiology* **155**, 268–278 (2009).
30. Tatsumi, H., Kano, K. & Ikeda, T. Kinetic Analysis of Fast Hydrogenase Reaction of Desulfovibrio v ulgaris Cells in the Presence of Exogenous Electron Acceptors. *J. Phys. Chem. B* **104**, 12079–12083 (2000).
31. González-Aragón, D., Ariza, J. & Villalba, J. M. Dicoumarol impairs mitochondrial electron transport and pyrimidine biosynthesis in human myeloid leukemia HL-60 cells. *Biochem. Pharmacol.* **73**, 427–439 (2007).
32. Davis, L. H. & Kauffman, F. C. Metabolism via the pentose phosphate pathway in rat pheochromocytoma PC12 cells: effects of nerve growth factor and 6-aminonicotinamide. *Neurochem. Res.* **12**, 521–527 (1987).
33. Zhao, J., Wang, Z., Fu, C., Wang, M. & He, Q. The mediated electrochemical method for rapid fermentation ability assessment. *Electroanal.* **20**, 1587–1592 (2008).
34. Kumar, S. & Acharya, S. K. 2, 6-Dichloro-phenol indophenol prevents switch-over of electrons between the cyanide-sensitive and-insensitive pathway of the mitochondrial electron transport chain in the presence of inhibitors. *Anal. Biochem.* **268**, 89–93 (1999).
35. Heiskanen, A. *et al.* Mediator-assisted simultaneous probing of cytosolic and mitochondrial redox activity in living cells. *Anal. Biochem.* **384**, 11–19 (2009).
36. Lesuisse, E. & Labbe, P. Iron reduction and trans plasma membrane electron transfer in the yeast *Saccharomyces cerevisiae*. *Plant Physiol.* **100**, 769–777 (1992).
37. Lesuisse, E., Casteras-Simon, M. & Labbe, P. Evidence for the Saccharomyces cerevisiae ferrireductase system being a multicomponent electron transport chain. *J. Biol. Chem.* **271**, 13578–13583 (1996).
38. Collier, A. C. & Pritsos, C. A. The mitochondrial uncoupler dicumarol disrupts the MTT assay. *Biochem. Pharm.* **66**, 281–287 (2003).
39. Ralser, M. *et al.* Dynamic rerouting of the carbohydrate flux is key to counteracting oxidative stress. *J. Biol.* **6**, 1–18, doi:10.1186/jbiol61 (2007).
40. Zuurbier, C. *et al.* Inhibition of the pentose phosphate pathway decreases ischemia–reperfusion-induced creatine kinase release in the heart. *Cardiovasc. Res.* **62**, 145–153 (2004).
41. Rashid, F., Horobin, R. W. & Williams, M. Predicting the behaviour and selectivity of fluorescent probes for lysosomes and related structures by means of structure-activity models. *Histochem. J.* **23**, 450–459 (1991).
42. Rashid, F. & Horobin, R. W. Interaction of molecular probes with living cells and tissues. Part 2. A structure-activity analysis of mitochondrial staining by cationic probes and a discussion of the synergistic nature of image-based and biochemical approaches. *Histochem. Cell Biol.* **94**, 303–308, doi:10.1007/BF00266632 (1990).
43. Roscoe, S. B., Rakow, N., Husberg, M. L. & McIntosh, L. H. Method of forming a pharmaceutical composition. US patent US20050065062 (2005).

44. Guo, J., Song, W., Ding, F., Zhang, J. & Sun, Z. Study on cytotoxicity and structure–activity relationship of HL-7702 cell exposed to naphthoquinones. *Environ. Toxicol. Pharmacol.* **33**, 408–413 (2012).
45. Rich, P. R. & Harper, R. Partition coefficients of quinones and hydroquinones and their relation to biochemical reactivity. *FEBS Lett.* **269**, 139–144 (1990).
46. Surmeian, M. *et al.* Distribution of methyl red on the water-organic liquid interface. *Anal. Lett.* **34**, 1421–1429 (2001).

Acknowledgments

We would like to thank James M. Nuttall (University of Sheffield, UK), Frédéric Barrière (Université de Rennes 1, France) and Wolfgang Schuhmann (Ruhr-Universität Bochum) for helpful discussions. We also thank the Marsden Fund, Royal Society of New Zealand (contract UOC 0605) and the Leverhulme Trust (ECF/2013-306) for funding.

Author contributions

K.H.B., A.J.D. and F.J.R. contributed equally to proposing the experimental concepts, planning the experiments and analysing the data. F.J.R. performed the experiments. All authors contributed equally to writing the manuscript.

Additional information

Competing financial interests: The authors declare no competing financial interests.

How to cite this article: Rawson, F.J., Downard, A.J. & Baronian, K.H. Electrochemical detection of intracellular and cell membrane redox systems in *Saccharomyces cerevisiae*. *Sci. Rep.* **4**, 5216; DOI:10.1038/srep05216 (2014).